RADIATION RESEARCH **176,** 415–424 (2011)
0033-7587/11 $15.00

DOI: 10.1667/RR2665.1

Impedance-Based Surveillance of Transient Permeability Changes in Coronary Endothelial Monolayers after Exposure to Ionizing Radiation

Erik F. Young[1] and Lubomir B. Smilenov

Center for Radiological Research, Columbia University College of Physicians and Surgeons, New York, New York

Young, E. F. and Smilenov, L. B. Impedance-Based Surveillance of Transient Permeability Changes in Coronary Endothelial Monolayers after Exposure to Ionizing Radiation. *Radiat. Res*. 176, 415–424 (2011).

The relative radiation sensitivities of the various compartments of the heart are poorly characterized. Cardiac fibrosis is a common side effect of radiotherapy, suggesting that endothelial barrier function is an important factor in radiation-induced pathology. We employed Electric Cell Substrate Impedance Sensing (ECIS) to assess cytoskeletal rearrangement, permeability changes and endothelial barrier function changes in response to radiation in studies of human coronary arterial endothelial cells (HCAECs). A 5-Gy dose of γ radiation resulted in a significant sixfold transient decrease in transmonolayer resistance 3 h postirradiation ($P = 0.001$). This decrease in resistance coincided with changes in fluorescent tracer flux ($P = 0.05$) and display of an actin bundling phenotype. After irradiation, decreases in wound healing ($P = 0.03$) and micromotion within the monolayer ($P = 0.02$) were also observed. Time-lapse video studies confirmed that the monolayer is dynamic and showed that cells are extruded from the monolayer at a higher frequency after irradiation. These findings suggest that perturbed endothelial barrier function in the heart can occur at lower doses of γ radiation than previously reported.

INTRODUCTION

Radiation-induced heart disease is of concern given the exposure of the heart not only in therapeutic management of breast cancer and Hodgkin's disease but also prophylaxis in prostate cancer patients to counter gynecomastia (*1, 2*). More recently, interest in the effects of occupational, exposure to low-dose radiation on the heart has increased (*3, 4*). At doses greater than 50 Gy, overt damage to the relatively radioresistant myocardium is seen (*5, 6*). However, at doses of approximately 2 Gy encountered in clinical fractionated radiotherapy, radiation-induced heart disease is believed to be a disorder of the endothelial cells in the heart.

Several aspects of normal vascular function are ablated by ionizing radiation. Normal function entails the ability of the vasculature to contract or relax in response to vasoactive hormones and cytokines as well as the ability to form a competent barrier that will resist thrombosis and respond to signals from the immune system. In response to injury or infection, normal endothelial immune response involves altered surface expression of selectins and several other adhesion molecules to facilitate rolling of leukocytes, which, after activation, extravasate where they then function (*7, 8*). Radiation can inappropriately activate this sequence of events, presumably in response to oxidative damage induced at the site (*9*). Contraction and relaxation kinetics are altered in *ex vivo* experiments where sections of great vessels are irradiated (*10–12*). These mechanisms, involving nitric oxide, are important in maintenance of vascular tone (*13*). The contribution of prostanoid biology in the vascular radiation response is exemplified by the reduction in radiation-induced atherosclerotic plaque formation in the carotid arteries by COX2 inhibition (*14*). Thus prostanoid-dependent vascular contractility, prostanoid-independent vascular contractility, and immune response are all ablated by radiation.

In addition to effects on contractility and paracrine signaling, radiation also causes overt changes in barrier function to the extent that dyes and tracers can flow out of the vasculature after irradiation (*15*). The ramifications of radiation-induced barrier failure in smaller vessels has been studied, and the result appears to be a modified immune response resulting in the deposition and remodeling of the extracellular matrix, leading to fibrosis (*16, 17*). In the heart, ectopic remodeling of the matrix will have deleterious effects on cardiac function (*18, 19*). Failure of this barrier can inappropriately admit soluble factors from blood that can then serve as stimulants for leukocyte homing and smooth muscle cell proliferation, resulting in an atherosclerotic lesion (*14, 20, 21*). Such lesions are also induced in young radiotherapy patients with no pre-existing athero-

[1]Address for correspondence: Columbia University, 630 W. 168th Street, VC11-204, New York, NY 10032; e-mail: efy1@columbia.edu

sclerosis (*22*). The mechanism underlying the iatrogenic generation of both these lesions and fibrosis is of great interest.

At the molecular level, the initiation of endothelial cell death in response to radiation is concomitant with the activation of stress-activated kinase cascades, including the transduction of a radiation damage signal via p38 and JNK (*23*). In primary cells from the aorta, radiation-induced apoptosis is mediated by NF-κB signaling (*24*). In spite of this assembled body of work, the details of endothelial dysfunction in radiation-induced heart disease remain unclear. Further, the relative sensitivities of cardiac substructures to radiation damage have not been determined. In addressing these questions, we considered that endothelium from bovine adrenals exhibits a compromised ability to organize the cytoskeleton into a migration-competent apparatus when assessed 24 h after irradiation, producing a delay in wound closure that is also seen in dermal microvascular endothelial cells (DMVECs) (*25, 26*). Furthermore, at least one type of endothelial cells are known to respond to radiation with a robust Rho-mediated cytoskeletal rearrangement at doses of 20 Gy with relatively rapid kinetics of 10–30 min (*27*). A key point of study, then, is the examination of very subtle changes in barrier function and cell dynamics of coronary endothelium in response to lower doses of radiation between 0 and 5 Gy.

Measurement of electrical impedance across layers of cells can provide information regarding cellular morphology and barrier function (*28, 29*). For this reason and several others, we selected Electric Cell Substrate Impedance Sensing (ECIS) as an investigative tool. First, the technique is non-invasive owing to the very small amplitude of interrogating currents employed (<40 μA/cm^2). Second, the method is exquisitely sensitive, successfully reporting not only micromovement in confluent monolayers but also cellular changes in response to the fluctuations in ambient CO_2 of $\pm 0.5\%$ in tissue culture incubators (*30, 31*). When cell monolayers are seeded on gold planar arrays, a variety of biological processes can be assessed, including spreading, adhesion, migration and transgression of the monolayer by invasive, heterotypic cells (*32, 33*). The transmonolayer impedance of endothelial cells in particular responds robustly when treated with compounds known to perturb endothelial barrier function, including thrombin, histamine and calcium chelating agents, and a model has been tested allowing for electronic assessment of permeability changes in response to these stimuli (*34–36*). Moreover, this technology allows for continuous cell monitoring over tens of hours, which is a unique and powerful feature of this experimental approach. The goal of this work was to assess radiation-induced barrier changes in human coronary endothelial monolayers using an impedance-based micromorphometry technique. Particular attention was paid to rearrangements of the cytoskeleton that could alter the barrier function of the tissue.

MATERIALS AND METHODS

Cell Culture

Human coronary arterial endothelial cells (HCAECs) were obtained from Lonza (Rockville, ME) as either actively growing cultures or frozen ampoules. Cells were subcultured in a modified form of commercially available medium in which all additives were used with the exception of hydrocortisone (EGM-2-MV Bullet Kit, Lonza, Rockville, ME).

Conventional cultureware was coated with collagen by preparing a 30-μg/ml solution of Rat Tail Col I (BD) in water and overlaying the cultureware with the coating solution for 1 h at 37°C prior to seeding cultures on the growth surface. Cells were maintained in humidified incubator at 37°C and 95% air/5% CO_2 and were fed three times per week.

Irradiation

Cells were transported to a nearby Gammacell 40 apparatus (Atomic Energy, Ontario, Canada) that delivered ^{137}Cs γ rays at a dose rate of 0.79 Gy/min. Cultureware was insulated during transport and irradiation to limit the effects of temperature changes.

Electric Cell Substrate Impedance Sensing

All measurements were performed using an Applied Biophysics ECIS-Zθ instrument that allows measurement of complex impedance of cell monolayers over a range of frequencies. For the impedance-related experiments, ''8W10E+'' type ECIS arrays (Applied Biophysics, Troy, NY) were coated with extracellular matrix substrate by addition of 400 μl of a Rat Tail collagen 1 solution to each well. This array type (see Fig. 1A) allows for measurements at 40 regularly spaced working electrodes over the 0.8-cm^2 surface of the culture with an interdigitated array of counterelectrodes forming the other terminus of the circuit. Collagen densities were 50 μg/cm^2 culture area, and arrays were incubated at 37°C for 1 h. After coating, the wells were aspirated dry and blocked with a 400-μl volume of a 1% w/v solution of bovine serum albumin (BSA) in PBS. Blocking was also carried out for 1 h at 37°C. After blocking, wells were aspirated dry and HCAECs were seeded on gold planar electrodes at a density of 75×10^3 cells/cm^2 in medium permitting an almost confluent density at the outset of the experiment. Impedance measurements made at 11 frequencies with an ECIS-Zθ instrument at 5-min intervals and logged on a command laptop computer running proprietary ECIS software.

For wound recovery experiments, ''8W1E'' type ECIS arrays were used. This second type of array allows for measurements at a single, central point (Fig. 1A, lower portion) with a working electrode 250 μm in diameter with a larger surrounding counterelectrode completing the circuit. Cells were allowed to mature to competent monolayers and were then subjected to an alternating current with an amplitude of 1400 μA for 20 s at a frequency of 60 kHz, effectively denuding the electrode surface (~0.05 mm^2) of cells. Impedance measurements then resumed, permitting surveillance of the rate at which cells migrated over the freshly denuded surface, allowing the monitoring of wound closure.

A survey of micromotion was conducted by investigating cells on ''8W1E'' electrodes for 5 h after wound recovery 5 h after the initial irradiation. Ohmic resistance values recorded at 4000 Hz on this single point array reflect the coverage of a 250-μm-diameter region by the cells residing in the monolayer. These acquired values were compiled, and a micromotion index (*mmi*) was calculated using the sum of the absolute values of differences between the data points. This index reflects the total swept distance of the recording trace and is described by Eq. (1) below, where R represents the resistance value in ohms/cm^2 at 5-min intervals.

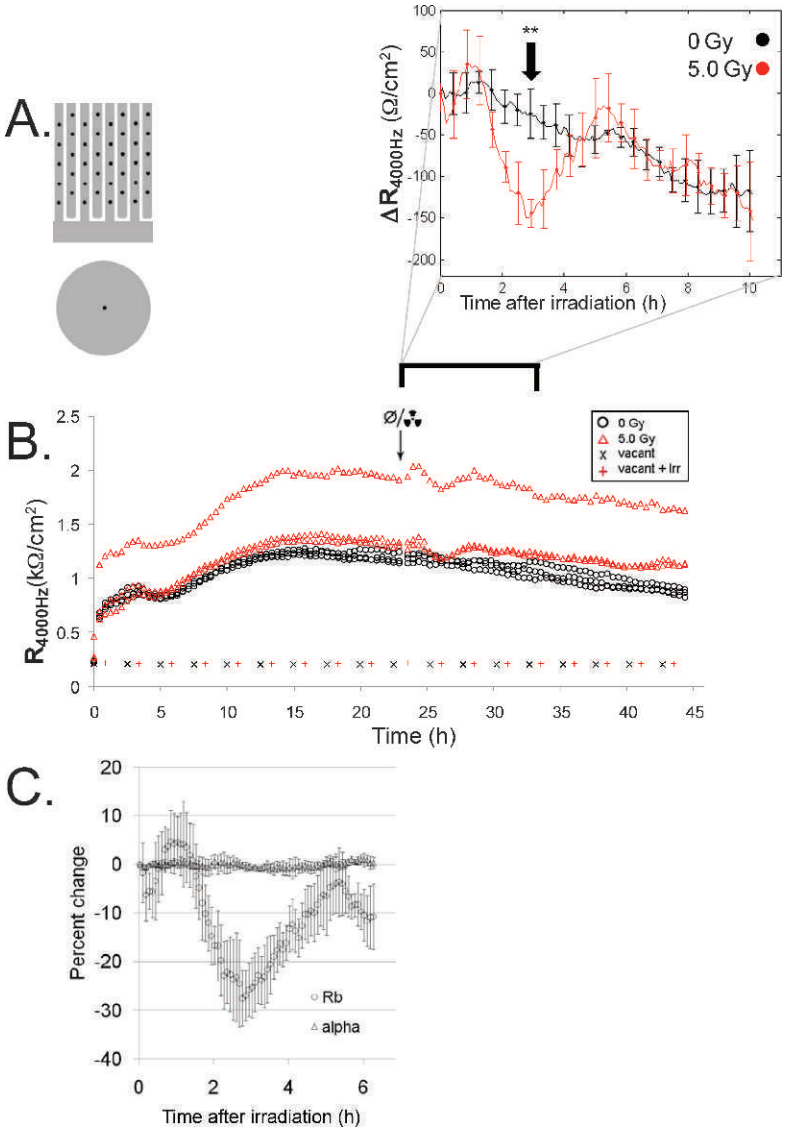

FIG. 1. Transmonolayer impedance measurement of irradiated HCAEC monolayers. For permeability recordings, cells were seeded on collagen-coated, planar electrode arrays depicted in the upper portion of panel A, and impedance measurements were made at 5-min intervals over 48 h. Cytoskeletal dynamics were measured using different arrays with the configuration shown in the lower portion of panel A. As shown in panel B, monolayers contact the array, spread and then seal into competent monolayers after 18–20 h, then decline. The change in resistance after irradiation is plotted (inset) with the average of technical triplicates and standard deviations shown. Three hours after irradiation, the difference between irradiated monolayers and sham-irradiated cells (**) was found to be statistically significant ($P = 0.001$). Modeling of impedance data from irradiated monolayers, shown in panel C, revealed that the modeling parameter α was largely unchanged, indicating that the change in monolayer impedance was predominantly attributable to paracellular changes reported by the parameter Rb. HCAEC monolayers exhibit a transient and statistically significant decrease in resistance 3 h after irradiation.

$$mmi = \frac{\sum_{i=2}^{n} |R_i - R_{(i-1)}|}{1000}.$$

Confocal Microscopy

Cells were cultured on collagen-coated glass cover slips and blocked as above at area-corrected seeding densities relative to culture on ECIS arrays. Wells were aspirated dry, washed with PBS, fixed by addition of 4% paraformaldehyde in PBS for 10 min, and then stored overnight in PBS at 4°C. The next day, cells were permeabilized by addition of 0.5% Triton X-100 in PBS for 5 min and then left in PBS for 10 min prior to staining. Cover slips were placed face down on a 97-μl volume of staining solution and incubated for 1 h at 37°C. Staining solution was comprised of 10% normal goat serum in PBS supplemented with a 1:40 dilution of Alexa488-conjugated phalloidin (Molecular Probes, Eugene, OR). After staining, cover slips were immersed in PBS three times before being allowed to destain in a 5-ml volume of PBS for a subsequent 10 min. Cover slips were then

mounted on 50-μl volumes of Lerner Aquamount aqueous mounting medium (Thermo Scientific, Kalamazoo, MI) prior to imaging. Confocal images were obtained using a Nikon C1 confocal scanning head coupled to a TE-2000-U microscope. An infinity-corrected Plan Fluor 40X extra long working distance objective with a numerical aperture of 0.6 was used. Data from the confocal sensor were captured with EZ C1 software generating 512 × 512-pixel images that were exported in TIFF format.

Lucifer Yellow Dye Flux

Transwell inserts with diameter of 12 mm and pore size of 0.4 μm (Costar, Corning, NY) were coated with collagen and blocked with BSA at area-corrected volumes and densities to permit comparable coating to those conditions used on ECIS arrays as described above. Cells were seeded at area-corrected densities and monolayers were allowed to mature on the porous substrates for 20 h, at which point cells were irradiated. Immediately after irradiation (or sham control treatment), 50 μl of a concentrated Lucifer Yellow solution was added to the lower compartment of the culture at a final concentration of 0.5 mg/ml. Samples of 10 μl were removed from the upper part of the culture at subsequent intervals and stored at 4°C until analysis. For fluorimetric analysis, a 1:20 dilution was made of a 5-μl portion of each sample in water, and this volume was subject to fluorimetry using a Synergy2 96-well plate reader under the command of Gen5 software (Biotek, Highland Park, VT). The reader was configured for excitation and emission wavelengths appropriate to Lucifer Yellow.

Statistical Treatment of Data

All assessments for statistical significance were two-tailed Student's *t* tests unless otherwise specified. Differences were deemed significant when acquired *P* values were equal to or less than 0.05.

RESULTS

Radiation-Induced Changes in Electrical Properties of Coronary Endothelial Monolayers

HCAECs were seeded in all experiments at a uniform density 75×10^3 cells/cm^2 on substrates that were coated with rat tail collagen I at a density of 50 μg/cm^2. To assess the effects of radiation on this coronary tissue, we employed ECIS technology and seeded cells on collagen-coated gold planar arrays optimized for surveillance of transmonolayer resistance and associated sealing and permeability. We observed an immediate and early development of resistance attributed to contact and spreading of the cells on the array surface (Fig. 1B). This process appeared to resolve by 4 h after seeding. The next phase, marked by a further increase of resistance, appeared to be sealing and maturation of lateral contacts. This maturation appeared to peak in a range of 18 to 22 h and was characteristic of several experiments using cells from three separate human donors. Finally, the electrical resistance of monolayers begins to decline over the remainder of the time course to values near the initial immature monolayer. We irradiated HCAEC monolayers with a dose of 5 Gy because this dose constituted the threshold of detection for cytoskeletal rearrangement in endothelial cells in a survey of irradiated endothelia in the literature (*27*). Higher doses of 10 and 20 Gy generated more robust rearrangements. When competent, mature monolayers are irradiated with 5 Gy, a small initial rise in the resistance values precedes a statistically significant ($P = 0.001$) drop in irradiated cells that appears at 3 h postirradiation (Fig. 1, inset).

Impedance-Based Structural Modeling of Coronary Endothelial Monolayers

A notable advantage of ECIS is the ability to electronically dissect the contribution of cellular shape to the resultant impedance. Multifrequency transmonolayer impedance measurements can be input into a model of monolayer structure that makes use of 0 and first-order Bessel transforms to dissect paracellular and cell-substrate interactions (*30*). Transmonolayer permeability in endothelial cells is known to be associated with changes in the Rb parameter of this model, giving a readout of paracellular conductance changes (*35*). We found that the Rb parameter was significantly altered after irradiation with 5 Gy and, more importantly, that the α parameter, associated with cell-substrate interaction, was not altered as a result of this treatment (Fig. 1C).

Radiation-Induced Cytoskeletal Changes

Cytoskeletal rearrangement is known to occur in endothelial cells exposed to 15–20 Gy (*27*). We conducted a survey of the cytoskeleton in HCAECs at various times after irradiation, including 3 h, at which the impedance measurements suggested that such a rearrangement might take place. In comparison with sham-irradiated controls, phaolloidin-stained preparations of irradiated HCAECs showed cells with a slightly more polygonal shape with bundling of actin fibers at the periphery of the cells and a notable retraction from neighboring cells (Fig. 2A). In a separate experiment, HCAEC monolayers were followed over 6 h; the prominence of this phenotype was greatest in 3-h samples before resolving thereafter (Fig. 2B). Taken together, these findings reveal a transient rearrangement of the cytoskeleton in response to radiation that coincides with a loss in barrier function as assessed by ECIS.

Radiation-Induced Changes in Monolayer Permeability

To further confirm that cytoskeletal rearrangements were coincident with changes in monolayer permeability as predicted by the impedance measurements, the flux of a neutral, fluorescent tracer dye across the monolayer was measured. Cells were seeded on collagen-coated, porous substrates and allowed to mature into monolayers that were irradiated and monitored over 4 h. Fluorescent dye concentrations increased in the upper compartment over the time course, with vacant inserts always permitting greater amounts of dye across the substrate. While little to no difference in dye concentration in the upper compartment of the culture system was seen at 2 h, a statistically

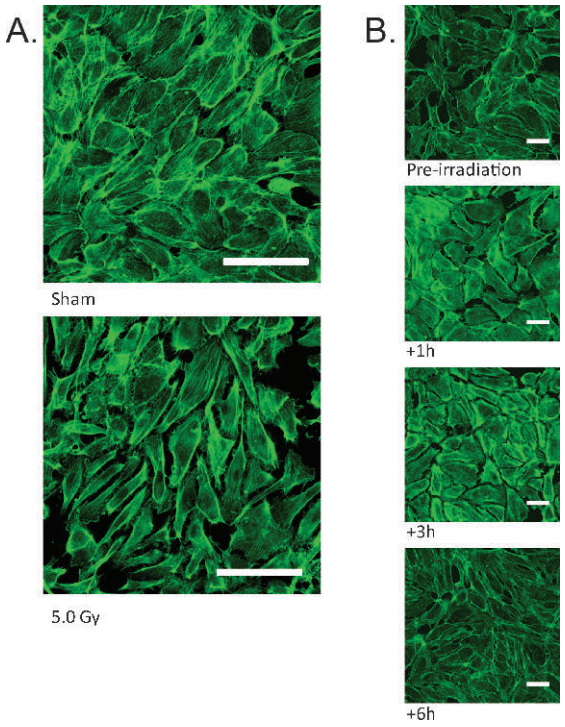

FIG. 2. Cytoskeletal rearrangement in HCAEC monolayers after irradiation. Cells were grown on collagen-coated glass cover slips and allowed to mature into monolayers for 18–20 h. Mature monolayers were irradiated at a dose of 5 Gy and were then fixed and stained with fluorescent phalloidin. Three hours after irradiation, HCAECs exhibited a boxy, polygonal phenotype with larger gaps between the cytoskeletons of neighboring cells compared to sham-irradiated controls as seen in panel A. When irradiated HCAECs were examined over time as shown in panel B, this phenotype was prominent at 3 h after irradiation and resolved by 6 h after irradiation. Cytoskeletal rearrangements correspond to temporal changes in transmonolayer permeability. Scale bars = 100 μm in panel A and 50 μm in panel B.

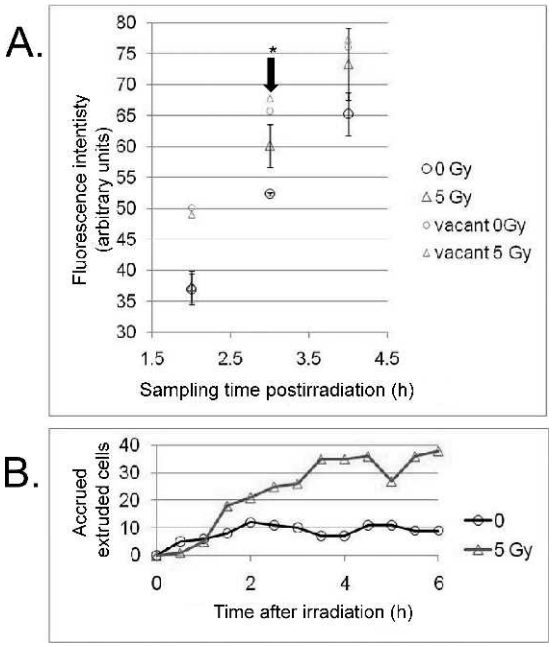

FIG. 3. Contributions to altered barrier function in HCAEC monolayers. Cells were seeded on a collagen-coated porous substrate and allowed to mature, then irradiated with 5 Gy of γ radiation. The diffusion of a low-molecular-weight neutral, fluorescent dye across monolayers was monitored, and the means of technical triplicates are shown with standard deviations. Compared to sham-irradiated monolayers, the flux of the dye was significantly increased ($P = 0.05$) at 3 h postirradiation (panel A). Intermittent cell detachment observed in fluorescence microscopy was assessed using video time-lapse microscopy (Supplementary Information; http://dx.doi.org/10.1667/RR2665.1.S2, http://dx.doi.org/10.1667/RR2665.1.S3, http://dx.doi.org/10.1667/RR2665.1.S4). Images were captured at regular intervals over a span of 1 h prior to irradiation and over the subsequent 24 h. Accrual of extruded, refractile cells from the monolayer was monitored; the increase in their numbers is plotted in panel B. The altered electrical signature after irradiation is an amalgam of both permeability changes and the departure of cells from the substrate.

significant increase in permeability to the dye was seen at 3 h postirradiation (Fig. 3A, $n = 3$; $P = 0.05$).

Time-Lapse Live Imaging Experiments

In all studies on collagen-coated glass substrates, we observed intermittent cell loss from the monolayer. This was initially attributed to disturbance during washing, fixation and staining. Based on results from time-lapse live imaging experiments, we believe these cells to be representative of a minority population that intermittently detaches in the course of culture (Supplementary Information; http://dx.doi.org/10.1667/RR2665.1.S1, http://dx.doi.org/10.1667/RR2665.1.S2, http://dx.doi.org/10.1667/RR2665.1.S3, http://dx.doi.org/10.1667/RR2665.1.S4). Also evident in videos was the extrusion of dead cells from the monolayer with concomitant closure of the monolayer by surrounding cells. This was a satisfying result that corroborated the finding of intermittent extrusion of cells seen in immunofluorescence microscopy studies. This intermittent extrusion of endothelial cells comprising turnover in the monolayer has been observed previously in primary culture (*37*). The accrual of these dead cells was seen to increase gradually over time in both irradiated monolayers and sham controls. In some instances, extruded cells were able to spread and reintegrate into the underlying monolayer again. The increase in accrued, extruded cells was greater in irradiated cells, with the onset of accrual beginning at 1.5 h and stabilizing at 3.5 h after irradiation (Fig. 3B). Other studies of irradiated endothelial cells from the lung showed a marked depolymerization of the actin cytoskeleton with a resultant pulmonary edema (*38–40*). In contrast, we found that coronary endothelial monolayers remained ostensibly intact when assessed with time-lapse light microscopy with no obvious retraction of cells from one another or visible gaps appearing between cells. Together, the impedance findings, microscopy and videos suggest that the transient loss in transmonolayer resistance is an amalgam of cytoskeletal rearrangement and increased cell extrusion from the monolayer.

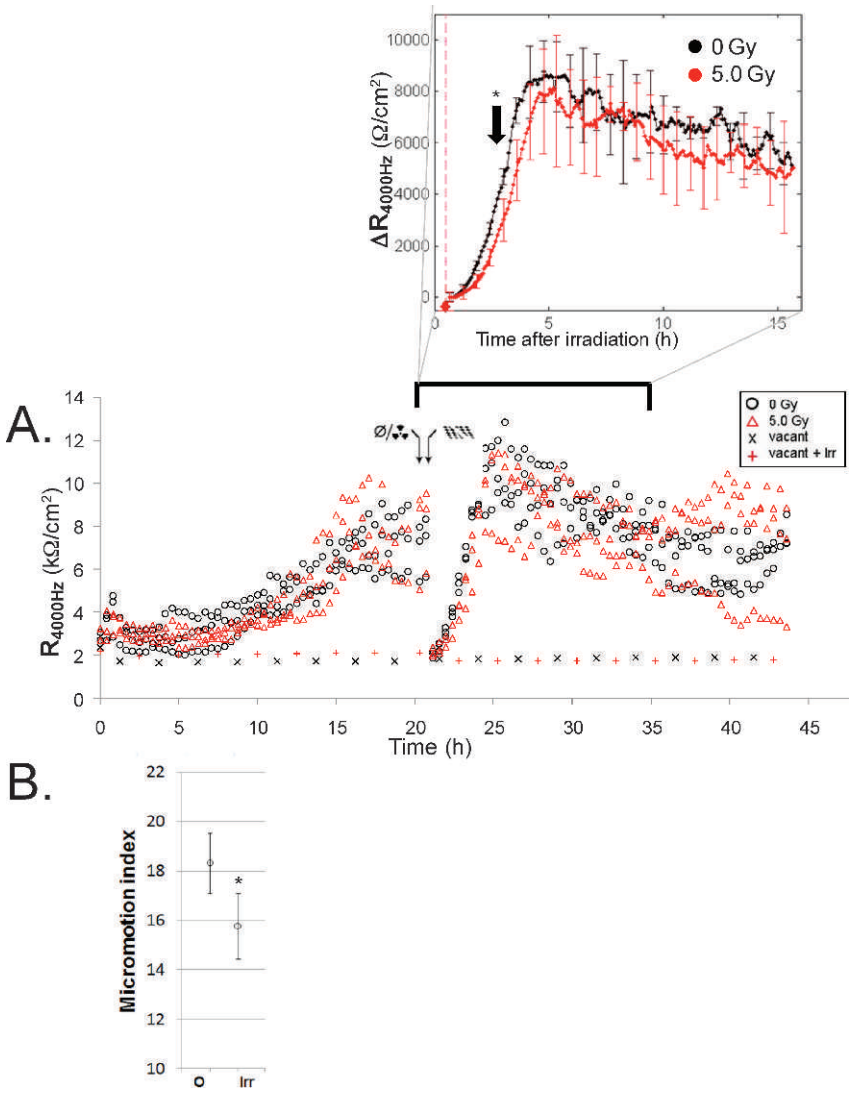

FIG. 4. Wound healing kinetics and micromotion in irradiated HCAEC monolayers. Cells were seeded on collagen-coated single-point gold planar array electrodes and impedance measurements were made over 45 h as shown in panel A. Monolayers were irradiated with 5 Gy of γ rays and then returned to standard culture for 30 min period prior to electrical creation of a wound. The change in resistance after irradiation is shown normalized relative to the lowest resistance value immediately after wounding (inset). The averages of technical triplicates with standard deviations are shown. Three hours after irradiation, the difference in resistance between the irradiated and sham-irradiated cells (*) was found to be statistically significant ($P = 0.03$). Panel B: Results of a comparison of calculated micromotion indices (*mmi*) using data from 10–15 h after irradiation. Informed by the radiation-induced deficit in wound closure, we found a statistically significant difference in a single-tailed Student's *t* test ($P = 0.02$). Irradiated HCAEC monolayers exhibited statistically significant delays in both wound healing and micromotion.

Radiation-Induced Changes in Cell Migration

We sought to further characterize cytoskeletal dynamics in HCAEC monolayers by conducting a wounding experiment on single-point ECIS arrays with a single 250-μm-diameter working electrode from which the interrogating electrical current originates, then passes through the monolayer and finally reaches the surrounding counter-electrode (Fig. 1A, lower portion). Again, monolayers were seen to mature when measured electrically. Given that the measurements were made at a single 0.05-mm^2 point instead of at 40 regularly spaced points over a 0.8-cm^2 area, the maturation was reported by a more irregular trace (Fig. 4A) compared with the resistance data presented in Fig. 1. Mature monolayers were irradiated with 5 Gy of γ rays as before, but after 30 min, monolayers were electrically removed from the central working electrode by driving 1400 μA at 60 kHz through the circuit for 20 s. This bolus of energy killed and removed cells from the electrode. The kinetics of wound closure over the electrode was reported

electrically. Irradiated cells were seen to lag behind sham-irradiated controls in wound closure, and, when assessed 3 h after irradiation, the difference between the two conditions was statistically significant (Fig. 4, inset, $n = 3$; $P = 0.03$).

After completion of the wound closure process, monolayer resistance was seen to return to values similar to preirradiation levels, and the recorded resistance values diminished slowly over the remainder of the time course as seen before. In this period, micromotion of cells transiting the 250-μm-diameter working electrode was recorded by examining fluctuation in the resistance of the monolayers. Ohmic resistance values acquired at 5-min intervals over a 5-h period spanning 10–15 h after irradiation were used to create a micromotion index (*mmi*) as described in the Materials and Methods. Given our suspicion that cytoskeletal dynamics were somehow compromised by radiation, we assessed the significance of the difference in calculated *mmi* values and found them to be statistically significant in a single-tailed Student's *t* test (Fig. 4B; $n = 3$; $P = 0.02$). Thus cytoskeletal dynamics assessed by dynamic motion in the monolayer is ablated by radiation, and wound closure is delayed as well.

DISCUSSION

Several studies have shown that endothelial function is compromised after doses of radiation over 15 Gy. These studies include demonstrations of perturbed barrier function, compromised transduction of relaxation signals, and altered prostanoid biology (*9–14*). Since the relative sensitivities of cardiac substructures to radiation damage have not been assessed the details of endothelial dysfunction in radiation-induced heart disease remain unclear, we studied the coronary endothelium. We investigated the changes in coronary endothelial function using ECIS. This is a unique, highly sensitive technology that allows us to monitor changes in live cell monolayers for days after irradiation.

The transmonolayer resistance measurements in our studies are made at 4 kHz and represent only the ohmic component of impedance for simplicity. We chose 4 kHz because this frequency exhibits the greatest response seen in a multifrequency spectrum for our monolayers in comparisons of early and mature monolayers. This frequency also permits comparison of our findings to a considerable number of ECIS-related publications dealing with endothelial biology where the same frequency is employed (*41, 42*). After irradiation, we observed changes in the transmonolayer impedance of HCAEC monolayers. These changes represent a compound response comprised of cytoskeletal rearrangements as seen in immunofluorescence surveys, increased monolayer permeability reported both electrically and in Lucifer Yellow flux studies, and increased extrusion of cells from the monolayer as seen in time-lapse imaging studies.

The significant and unique aspects of this work are the kinetics and morphometry of radiation-induced cytoskeletal rearrangement in an intact monolayer of HCAECs in response to a dose of γ radiation. Given our sensitive methodology, this rearrangement becomes discernible at much lower doses than those already used to investigate this response in other endothelia. We found that, 3 h after a 5-Gy dose, a transient loss of transmonolayer resistance occurred in irradiated samples and that this resolved over a subsequent 1–2-h period. This drop in resistance was coincident with the rearrangement of the actin cytoskeleton in similar preparations when the status of the cytoskeleton was analyzed by confocal microscopy. We also found that HCAECs exhibited delayed wound closure when wounded 30 min after irradiation and that the micromotion of these cells over a 250-μm-diameter electrode was reduced when a 5-h segment of the recording was assessed for this parameter. Together, these findings indicate that HCAECs have an altered cytoskeletal biology after exposure to ionizing radiation. Since reduction in transendothelial resistance is generally associated with increased permeability (*34, 35*), we believe that the more immediate and transient loss in resistance we observed is conducive to fibrosis and atherogenesis in the coronoary circulation.

The limitations of the study include its restriction to a two-dimensional analysis format and the induction of stress in the primary cells we used as a result of subculture outside their normal environment. The commercially available HCAECs halted division and senesced 10 to 14 days after procurement and culture. These stresses could have an impact the nature of the response we observed.

The strengths of the study include the use of ECIS technology, which made lengthy recordings of the monolayers possible. The modeling component of the instrumentation allows for angstrom-scale measurements of the compartment between the cells and the collagen-coated substrate (*30*). The ECIS method also permits a unique measurement of the micromotion parameter, providing information on the motility of resident cells in the endothelial monolayers and, indirectly, the ability of the cells to manipulate their cytoskeleton in the process of locomotion. Our use of primary HCAECs allowed a particularly useful insight into this important cardiac substructure.

Our findings in coronary endothelium differ from other studies in which cells were obtained from other tissues. Pulmonary endothelium is known to undergo a depolymerization of the actin cytoskeleton, and this results in a physiologically significant increase in the wet weight of the lungs as edema accrues (*39, 40*). Gabrys *et al*. (*27*) demonstrated that a Rho-mediated, radiation-induced cytoskeletal rearrangement occurred in certain endothelial cells and that only in DMVECs was this process independent of p38. Others found that both p38 and JNK were activated in irradiated human umbilical vein endothelial cells (HUVECs) (*23*). Endothelial cells will undoubtedly have

different characteristics based on the tissue from which they are obtained. DMVECs will have a role in thermoregulation, for example, which is not relevant for HUVECs. Endothelial cells from bovine adrenal glands (BAECs) are exposed to a very different endocrine milieu compared to the endothelium in the blood-brain barrier. Similarly, coronary endothelium resides in a physiologically unique location that has one of the highest oxygen consumption sites in the body. In a comparison between various endothelial subtypes plated on laminin, only HCAECs did not exhibit a statistically significant increase in proliferation (*43*). It is not unreasonable, therefore, to expect a different radiation response from this endothelium given the increased turbulence, shear and incessant flexion of the adjacent epicardium.

The kinetics of our observed radiation-induced cytoskeletal rearrangements differs from the effects observed in other studies of endothelial tissue *ex vivo*. Immediate and early responses to radiation have been observed with kinetics of less than 30 min. Such rapid responses include conversion of sphingomyelin to ceramide and the induction of endothelin transcripts (*44, 45*). The differences in kinetics could arise from the endothelial cell type as discussed above or from a difference in the extracellular matrix (ECM).

Several different radiation biology studies indicate that the ECM is an important factor in the biology of endothelial cells. A number of studies of endothelia indicate that there is an interplay between radiation-induced damage and survival signaling from matrix through ECM receptors (integrins) along the PI3K-Akt axis (*43, 46–48*). All of the work conducted in this study involved HCAECs plated on substrates coated with collagen I, so the migration and signaling we observed was mediated primarily by $\alpha1\beta1$ and $\alpha2\beta1$ integrins. Adhesion to and migration on denatured collagen (gelatin) or vitronectin is mediated by $\alpha v\beta3$, which is upregulated in endothelium that is localized near tumors or wound tissue (*49, 50*). The surface expression of integrins in HCAECs was not measured here, but given that HCAECs are dissociated from their resident tissue and are in culture *ex vivo*, it is likely that $\alpha v\beta3$ is expressed on the surface of these cells. The magnitude or kinetics of our observed response may vary with the composition of the ECM on which the monolayer is seeded.

Endothelial barrier function is compromised after irradiation, and this can be attributed to paracellular or transcellular communication between the blood and tissue. More definitive results have been seen in the endothelial barrier in the brain, where the paracellular pathway has been found to be modulated after a single dose of 20 Gy (*51*). In the heart and in irradiated tumor vasculature, findings support transcellular communication between tissue and blood after fractionated radiotherapy or a single dose of 10–13 Gy (*52, 53*). Paracellular communication would seem to be more relevant at doses where overt killing of the endothelium is observed (*54–56*), and the resultant access to ECM in the context of dysfunctional endothelium could account for the accrual of von Willebrand factor by means of collagen binding domains of this platelet aggregating factor (*57*). Our findings suggest that lower doses where endothelial cells are not killed could still induce transient communication between the blood and myocardium.

Finally, it is important to consider that the coronary endothelium is a component of a complete cardiopulmonary system. The ultimate detrimental effect of radiation-induced heart disease is reduction of cardiac function. Irradiation of the thorax for diagnostic or therapeutic reasons includes exposure of the lungs, myocardium, pericardium, great vessels and coronary circulation. Radiation-induced effects on any of these components can cause feedback into others in a decompensating feedback loop, resulting in failure (*58*). We anticipate that future studies will further detail the role of endothelial dysfunction in radiation-induced heart disease and that additional sub-compartments of the heart will be assessed for their respective radiation sensitivities.

ACKNOWLEDGMENTS

The authors are deeply indebted to I. Giaver, C. Keese and Applied Biophysics for access to an ECIS instrument, without which this work would not have been possible. The authors are also thankful to S. Amundsen and S. Ghandhi for helpful discussions and to T. Templin for assistance with the assembly of the manuscript. This work was supported with funding from the Department of Energy (DEPS0208ER0820) and NASA (NNX07AT41G).

Received: April 28, 2011; accepted July 27, 2011; published online: August 22, 2011

REFERENCES

1. Basavaraju SR, Easterly CE. Pathophysiological effects of radiation on atherosclerosis development and progression, and the incidence of cardiovascular complications. Med Phys 2002; 29:2391–403.
2. Nieder C, Pawinski A, Andratschke NH, Molls M. Does prophylactic breast irradiation in patients with prostate cancer influence cardiac toxicity? J Natl Cancer Inst 2007; 99:1646–7.
3. Darby SC, Cutter DJ, Boerma M, Constine LS, Fajardo LF, Kodama K, et al. Radiation-related heart disease: current knowledge and future prospects. Int J Radiat Oncol Biol Phys 2010; 76:656–65.
4. Little MP, Gola A, Tzoulaki I. A model of cardiovascular disease giving a plausible mechanism for the effect of fractionated low-dose ionizing radiation exposure. PLoS Comput Biol 2009; 5:e1000539.
5. McChesney SL, Gillette EL, Powers BE. Radiation-induced cardiomyopathy in the dog. Radiat Res 1988; 113:120–32.
6. Powers BE, Thames HD, Gillette EL. Long-term adverse effects of radiation inhibition of restenosis: radiation injury to the aorta and branch arteries in a canine model. Int J Radiat Oncol Biol Phys 1999; 45:753–9.
7. Quarmby S, Hunter RD, Kumar S. Irradiation induced expression of CD31, ICAM-1 and VCAM-1 in human microvascular endothelial cells. Anticancer Res 2000; 20:3375–81.
8. Quarmby S, Kumar P, Wang J, Macro JA, Hutchinson JJ, Hunter RD, et al. Irradiation induces upregulation of CD31 in human endothelial cells. Arterioscler Thromb Vasc Biol 1999; 19:588–97.
9. Allen JB, Sagerman RH, Stuart MJ. Irradiation decreases vascular

prostacyclin formation with no concomitant effect on platelet thromboxane production. Lancet 1981; 2(8257):1193–6.

10. Menendez JC, Casanova D, Amado JA, Salas E, Garcia-Unzueta MT, Fernandez F, et al. Effects of radiation on endothelial function. Int J Radiat Oncol Biol Phys 1998; 41:905–13.
11. Qi F, Sugihara T, Hattori Y, Yamamoto Y, Kanno M, Abe K. Functional and morphological damage of endothelium in rabbit ear artery following irradiation with cobalt60. Br J Pharmacol 1998; 123:653–60.
12. Soloviev A, Prudnikov I, Tsyvkin V, Tishkin S, Kyrychenko S, Zelensky S, et al. Electrophysiological and contractile evidence of the ability of human mesenchymal stromal cells to correct vascular malfunction in rats after ionizing irradiation. J Physiol Sci 2010; 60:161–72.
13. Furchgott RF, Vanhoutte PM. Endothelium-derived relaxing and contracting factors. FASEB J 1989; 3:2007–18.
14. Aarnoudse MW, Lamberts HB, Dijk F, Vos J, de Vries AJ. Monocytes and radiation-induced atheromatosis in rabbits. Virchows Arch B Cell Pathol Incl Mol Pathol 1984; 47:211–6.
15. Jolles B, Harrison RG. Radiation skin reaction and depletion and restoration of body immune response. Nature 1963; 198:1216–7.
16. Baker DG, Krochak RJ. The response of the microvascular system to radiation: a review. Cancer Invest 1989; 7:287–94.
17. Griem ML, Robotewskyj A, Nagel RH. Potential vascular damage from radiation in the space environment. Adv Space Res 1994; 14:555–63.
18. Caulfield JB, Norton P, Weaver RD. Cardiac dilatation associated with collagen alterations. Mol Cell Biochem 1992; 118:171–9.
19. Kim HE, Dalal SS, Young E, Legato MJ, Weisfeldt ML, D'Armiento J. Disruption of the myocardial extracellular matrix leads to cardiac dysfunction. J Clin Invest 2000; 106:857–66.
20. Hoving S, Heeneman S, Gijbels MJ, te Poele JA, Bolla M, Pol JF, et al. NO-donating aspirin and aspirin partially inhibit age-related atherosclerosis but not radiation-induced atherosclerosis in ApoE null mice. PLoS One 2010; 5:e12874.
21. Hoving S, Heeneman S, Gijbels MJ, te Poele JA, Russell NS, Daemen MJ, et al. Single-dose and fractionated irradiation promote initiation and progression of atherosclerosis and induce an inflammatory plaque phenotype in ApoE(–/–) mice. Int J Radiat Oncol Biol Phys 2008; 71:848–57.
22. Huff H, Sanders EM. Coronary-artery occlusion after radiation. N Engl J Med 1972; 286:780.
23. Kumar P, Miller AI, Polverini PJ. p38 MAPK mediates gamma-irradiation-induced endothelial cell apoptosis, and vascular endothelial growth factor protects endothelial cells through the phosphoinositide 3-kinase-Akt-Bcl-2 pathway. J Biol Chem 2004; 279:43352–60.
24. Natarajan M, Mohan S, Konopinski R, Otto RA, Herman TS. Induced telomerase activity in primary aortic endothelial cells by low-LET gamma-radiation is mediated through NF-kappaB activation. Br J Radiol 2008; 81:711–20.
25. Scharpfenecker M, Kruse JJ, Sprong D, Russell NS, Ten Dijke P, Stewart FA. Ionizing radiation shifts the PAI-1/ID-1 balance and activates notch signaling in endothelial cells. Int J Radiat Oncol Biol Phys 2009; 73:506–13.
26. Speidel MT, Holmquist B, Kassis AI, Humm JL, Berman RM, Atcher RW, et al. Morphological, biochemical, and molecular changes in endothelial cells after alpha-particle irradiation. Radiat Res 1993; 136:373–81.
27. Gabrys D, Greco O, Patel G, Prise KM, Tozer GM, Kanthou C. Radiation effects on the cytoskeleton of endothelial cells and endothelial monolayer permeability. Int J Radiat Oncol Biol Phys 2007; 69:1553–62.
28. Giaever I, Keese CR. Monitoring fibroblast behavior in tissue culture with an applied electric field. Proc Natl Acad Sci U S A 1984; 81:3761–4.
29. Giaever I, Keese CR. A morphological biosensor for mammalian cells. Nature 1993; 366:591–2.
30. Giaever I, Keese CR. Micromotion of mammalian cells measured electrically. Proc Natl Acad Sci U S A 1991; 88:7896–900.
31. Lo CM, Keese CR, Giaever I. pH changes in pulsed CO_2 incubators cause periodic changes in cell morphology. Exp Cell Res 1994; 213:391–7.
32. Keese CR, Bhawe K, Wegener J, Giaever I. Real-time impedance assay to follow the invasive activities of metastatic cells in culture. Biotechniques 2002; 33:842–4, 846, 848–50.
33. Keese CR, Wegener J, Walker SR, Giaever I. Electrical wound-healing assay for cells in vitro. Proc Natl Acad Sci U S A 2004; 101:1554–9.
34. Moy AB, Van Engelenhoven J, Bodmer J, Kamath J, Keese C, Giaever I, et al. Histamine and thrombin modulate endothelial focal adhesion through centripetal and centrifugal forces. J Clin Invest 1996; 97:1020–7.
35. Moy AB, Winter M, Kamath A, Blackwell K, Reyes G, Giaever I, et al. Histamine alters endothelial barrier function at cell-cell and cell-matrix sites. Am J Physiol Lung Cell Mol Physiol 2000; 278:L888–98.
36. Tiruppathi C, Malik AB, Del Vecchio PJ, Keese CR, Giaever I. Electrical method for detection of endothelial cell shape change in real time: assessment of endothelial barrier function. Proc Natl Acad Sci U S A 1992; 89:7919–23.
37. Schaefer HI, van 't Hooft FM, van der Laarse A. Growth characteristics of a permanent human endothelial cell line. In Vitro Cell Dev Biol 1992; 28A:465–7.
38. Evans ML, Graham MM, Mahler PA, Rasey JS. Changes in vascular permeability following thorax irradiation in the rat. Radiat Res 1986; 107:262–71.
39. Kantak SS, Diglio CA, Onoda JM. Low dose radiation-induced endothelial cell retraction. Int J Radiat Biol 1993; 64:319–28.
40. Onoda JM, Kantak SS, Diglio CA. Radiation induced endothelial cell retraction in vitro: correlation with acute pulmonary edema. Pathol Oncol Res 1999; 5:49–55.
41. Tiruppathi C, Freichel M, Vogel SM, Paria BC, Mehta D, Flockerzi V, et al. Impairment of store-operated Ca^{2+} entry in TRPC4(–/–) mice interferes with increase in lung microvascular permeability. Circ Res 2002; 91:70–6.
42. van Wetering S, van den Berk N, van Buul JD, Mul FP, Lommerse I, Mous R, et al. VCAM-1-mediated Rac signaling controls endothelial cell-cell contacts and leukocyte transmigration. Am J Physiol Cell Physiol 2003; 285:C343–52.
43. Rose RW, Grant DS, O'Hara MD, Williamson SK. The role of laminin-1 in the modulation of radiation damage in endothelial cells and differentiation. Radiat Res 1999; 152:14–28.
44. Kolesnick R, Fuks Z. Radiation and ceramide-induced apoptosis. Oncogene 2003; 22:5897–906.
45. Lanza V, Fadda P, Iannone C, Negri R. Low-dose ionizing radiation stimulates transcription and production of endothelin by human vein endothelial cells. Radiat Res 2007; 168:193–8.
46. Fuks Z, Vlodavsky I, Andreeff M, McLoughlin M, Haimovitz-Friedman A. Effects of extracellular matrix on the response of endothelial cells to radiation in vitro. Eur J Cancer 1992; 28A:725–31.
47. Cordes N, Blaese MA, Meineke V, Van Beuningen D. Ionizing radiation induces up-regulation of functional beta1-integrin in human lung tumour cell lines in vitro. Int J Radiat Biol 2002; 78:347–57.
48. Ning S, Chen Z, Dirks A, Husbeck B, Hsu M, Bedogni B, et al. Targeting integrins and PI3K/Akt-mediated signal transduction pathways enhances radiation-induced anti-angiogenesis. Radiat Res 2007; 168:125–33.
49. Brooks PC, Clark RA, Cheresh DA. Requirement of vascular

integrin alpha v beta 3 for angiogenesis. Science 1994; 264:569–71.

50. Brooks PC, Montgomery AM, Rosenfeld M, Reisfeld RA, Hu T, Klier G, et al. Integrin alpha v beta 3 antagonists promote tumor regression by inducing apoptosis of angiogenic blood vessels. Cell 1994; 79:1157–64.

51. Yuan H, Gaber MW, McColgan T, Naimark MD, Kiani MF, Merchant TE. Radiation-induced permeability and leukocyte adhesion in the rat blood-brain barrier: modulation with anti-ICAM-1 antibodies. Brain Res 2003; 969:59–69.

52. Debbage PL, Seidl S, Kreczy A, Hutzler P, Pavelka M, Lukas P. Vascular permeability and hyperpermeability in a murine adenocarcinoma after fractionated radiotherapy: an ultrastructural tracer study. Histochem Cell Biol 2000; 114:259–75.

53. Khan MY, Ohanian M. Radiation-induced cardiomyopathy: II. An electron microscopic study of myocardial microvasculature. Am J Pathol 1974; 74:125–36.

54. Boerma M, Zurcher C, Esveldt I, Schutte-Bart CI, Wondergem J. Histopathology of ventricles, coronary arteries and mast cell accumulation in transverse and longitudinal sections of the rat heart after irradiation. Oncol Rep 2004; 12:213–9.

55. Dimitrievich GS, Hausladen SL, Kuchnir FT, Griem ML. Radiation damage and subendothelial repair to rabbit ear chamber microvasculature. An in vivo and histologic study. Radiat Res 1977; 69:276–92.

56. Dimitrievich GS, Hausladen SL, Kuchnir FT, Griem ML, Yang VV, Stearner SP. Radiation damage and subendothelial repair to rabbit ear chamber microvasculature: an in vivo, histologic, and electron microscopic study. Bibl Anat 1977; 15:337–40.

57. Boerma M, Kruse JJ, van Loenen M, Klein HR, Bart CI, Zurcher C, et al. Increased deposition of von Willebrand factor in the rat heart after local ionizing irradiation. Strahlenther Onkol 2004; 180:109–16.

58. Schultz-Hector S. Radiation-induced heart disease: review of experimental data on dose response and pathogenesis. Int J Radiat Biol 1992; 61:149–60.